Saudi Journal of Biological Sciences 27 (2020) 2227–2237

Contents lists available at ScienceDirect

Saudi Journal of Biological Sciences

journal homepage: www.sciencedirect.com

Original article

Compounds isolated from *Euonymus spraguei* Hayata induce ossification through multiple pathways

Zuha Imtiyaz [a], Yi-Tzu Lin [a], Ut-Hang Cheong [b], Alagie Jassey [c], Hui-Kang Liu [d], Mei-Hsien Lee [a,b,e,*]

[a] Program in Clinical Drug Development of Herbal Medicine, College of Pharmacy, Taipei Medical University, Taipei 110, Taiwan
[b] Graduate Institute of Pharmacognosy, College of Pharmacy, Taipei Medical University, Taipei 110, Taiwan
[c] College of Medicine, Taipei Medical University, Taipei 110, Taiwan
[d] Division of Basic Chinese Medicine, National Research Institute of Chinese Medicine, Ministry of Health and Welfare, Taipei 112, Taiwan
[e] Center for Reproductive Medicine and Sciences, Taipei Medical University Hospital, Taipei 110, Taiwan

ARTICLE INFO

Article history:
Received 22 May 2020
Revised 18 June 2020
Accepted 22 June 2020
Available online 27 June 2020

Keywords:
Euonymus spraguei Hayata
Human osteoblast cells
Syringin
(−)-Epicatechin
Osteogenesis
Multi-target drugs

ABSTRACT

The process of bone metabolism includes catabolism of old or mature bone and anabolism of new bone, carried out by osteoclasts and osteoblasts respectively. Any imbalance in this process results in loss of bone mass or osteoporosis. Drugs available to combat osteoporosis have certain adverse effects and are unable to improve bone formation, hence identifying new agents to fulfil these therapeutic gaps is required. To expand the scope of potential agents that enhance bone formation, we identified *Euonymus spraguei* Hayata as a plant material that possesses robust osteogenic potential using human osteoblast cells. We isolated three compounds, syringaresinol (**1**), syringin (**2**), and (−)-epicatechin (**3**), from *E. spraguei*. Results demonstrated that syringin (**2**), and (−)-epicatechin (**3**), increased alkaline phosphatase activity significantly up to 131.01% and 130.67%, respectively; they also elevated mineral deposition with respective values of up to 139.39% and 138.33%. In addition, **2** and **3** modulated autophagy and the bone morphogenetic protein (BMP)-2 signaling pathway. Our findings demonstrated that **2** and **3** induced osteogenesis by targeting multiple pathways and therefore can be considered as potent multi-targeted drugs for bone formation against osteoporosis.

1. Introduction

Multi-target drugs (MTDs) interact with several biological substances. This type of approach is categorized under polypharmacology (Van der Schyf, 2011), and offers better efficacy, fewer side effects and decreased vulnerability to adaptive resistance (Sams-Dodd, 2005). Studies have shown that drugs interacting with multiple targets have a safer profile as compared to single-target drugs (Bolognesi and Cavalli, 2016). MTDs are well suited for complex diseases, which are controlled by several intrinsic and extrinsic factors acting together to drive the onset and progression of these diseases (Ramsay et al., 2018). Indeed, several MTDs are already on the market, such as lapatinib (Tykerb) for treating breast cancer (Morphy, 2010). Ladostigil, an MTD against neurodegenerative diseases has shown potential and is under investigation (Medicine, 2018). However, other complex metabolic diseases such as osteoporosis lack potent candidates for MTD development.

Osteoporosis constitutes one of the top health issues that hampers everyday functioning and poses a huge economic burden on the patients. The disease is characterized by weak and fragile bones, and low bone mineral density. Drugs available to combat osteoporosis are associated with adverse effects and are unable to improve the formation of new bone (Compston et al., 2019). More importantly, most of the osteoporosis drugs are also single-targeted. Therefore, the need to identify more effective drugs that have fewer side effects, can enhance bone formation, and target multiple pathways is dire. MTDs also have an advantage over the usage of multiple drugs for single pathological condition, as drug-drug interaction might have severe outcomes in some cases (Koeberle and Werz, 2014). For osteoporosis, co-administration of bisphosphonates with calcium supplements, or any oral medication containing divalent cation hinders the absorption of bisphosphonates and increases the risk of fracture in such patients

* Corresponding author at: Graduate Institute of Pharmacognosy, College of Pharmacy, Taipei Medical University, Taipei 110, Taiwan.
E-mail address: lmh@tmu.edu.tw (M.-H. Lee).
Peer review under responsibility of King Saud University.

Production and hosting by Elsevier

https://doi.org/10.1016/j.sjbs.2020.06.036
1319-562X/

(Rizzoli et al., 2011). Therefore, identifying active agents that have multiple molecular mechanisms involved in bone formation as their target is necessary.

Bone tissue undergoes remodeling throughout life to maintain its volume and mineral homeostasis (Hadjidakis and Androulakis, 2006). Several regulatory signals and interacting factors influence the process of bone cell differentiation and bone remodeling (Nishimura et al., 2008). At sites of remodeling, osteoblasts form new bone, whereas osteoclasts dissolve existing bone (Raggatt and Partridge, 2010). Osteoblasts undertake the production of bone matrix proteins, collagen type 1 (Col-1), which constitutes 90% of extracellular matrix (ECM) proteins. Bone sialoprotein (BSP), osteocalcin, osteonectin, and several other proteoglycans, are involved in the process of mineralization (Aubin and Triffitt, 2002). BMPs are closely involved in the expression of alkaline phosphatase (ALP), which also stimulates mineral deposition (Jimi et al., 2010; Kusumoto et al., 2002). Certain factors from osteoblasts control bone remodeling by influencing the rate of osteoclast formation. Binding of two factors produced by osteoblast, receptor activator of nuclear factor (NF)-κB ligand (RANKL) and osteoprotegerin (OPG) prevents the maturation and activation of osteoclast cells (Kobayashi et al., 2008). Autophagy is a cellular process involved in regulating the physiological function and survival of osteoblasts (Yin et al., 2019). This cellular process protects osteoblasts from the stress caused by toxic stimuli and superoxides (Nollet et al., 2014). All these essential molecules and their signaling mechanisms, together, contribute to the process of bone remodeling and thus can serve as suitable targets for therapeutic interventions against osteoporosis.

Plants are a rich source of secondary metabolites possessing medicinal properties. Their potential against neurodegeneration, cancer, oxidative stress, and skeletal disorders has been extensively established (Imtiyaz et al., 2019; Jolly et al., 2018). One such example is the plants from genus *Euonymus;* they are rich in medicinal properties and are also well known for their traditional uses. *E. alatus* is used traditionally against cancer, and is also used for pain relief and blood circulation in folk medicine (Sharma et al., 2012). Studies reported that *E. alatus* possesses anti-diabetic, anti-oxidant and anti-cancer potential (Cha et al., 2003; Chang et al., 2012). Other plants of the genus, like *E. japonicus,* possess anti-viral activity (Wei and Liu, 2016), and compounds isolated from this plant act as acetylcholinesterase inhibitors (Alarcón et al., 2015). *E. laxiflorus* is reported to inhibit α-glucosidase (Nguyen et al., 2017b) and α-amylase (Nguyen et al., 2017a). *E. fortunei* and *E. hederaceus* reportedly possesses anti-oxidant activity (Nguyen et al., 2019; Shao et al., 2016; Sun et al., 2009). During preliminary screening of certain native Taiwanese plants, we found that *E. spraguei* Hayata from family Calestraceae possesses osteogenic potential. A supporting study found that celastrol, a compound isolated from traditional Chinese medicine belonging to family Calestraceae significantly attenuates bone loss in mice with collagen-induced arthritis (Gan et al., 2015).

The present study aims to isolate and identify the active compounds of *E. spraguei,* followed by elucidating their osteogenic potential and possible underlying mechanisms using human osteoblast (HOb) cells as an experimental model.

2. Materials and methods

2.1. Extraction and compound isolation

Stems of *E. spraguei* (ES) were collected from Yuang-feng Mountain (Nantou, Taiwan) and the specimen was identified by Dr. Ih-Sheng Chen, College of Pharmacy, Kaohsiung Medical University (Kaohsiung, Taiwan). Following this an herbarium specimen voucher numbered M404 was assigned and deposited in the Graduate Institute of Pharmacognosy, Taipei Medical University (Taipei, Taiwan). Dried and crushed stems of ES (3.07 kg) were exhaustively extracted with 30 L of 95% ethanol for seven days (twice), and the resulting solution was vacuum evaporated to yield 96.08 g of a crude ES extract. Water was used to re-suspend ES extract followed by successive partitioning with *n*-hexane (H), ethyl acetate (E) and *n*-butanol (B), to yield ES-H (9.48 g), ES-E (3.81 g), ES-B (9.37 g) and aqueous (ES-A, 53.2 g) fractions.

The ES-E fraction was subjected to Diaion HP-20 (250–850 μm, Merck KGaA, Darmstadt, Germany) column chromatography using H_2O to MeOH as the mobile phase, and seven major sub-fractions (ES-E-1-1 ~ ES-E-1-7) were collected. ES-E-1-5 (0.51 g) and ES-E-1-6 (0.71 g) were combined and subjected to the Sepbox 2D-2000 system (Yang et al., 2015) (Sepiatec, Germany). This sample was transferred to an injection column and 18 fractions were collected using separation column I, a C-4 reverse-phase (RP) column. Further on, these fractions were transferred to solid-phase extraction (SPE) columns. Fractions present in each SPE column were then passed through separation column II, C-18 RP-high performance liquid chromatography (HPLC) for subsequent separation. Solvents different from those used during the first fractionation were used for elution. In total,176 individual sub-fractions (vials 1–176) were collected. ES-E-1-5,6-v11 was subsequently purified by an RP-HPLC column (Phenomenex Luna penta fluoro phenyl (PFP), 5 μm, 10 × 250 mm; Torrance, CA, USA) with 70% MeOH at a flow rate of 3 ml/min to collect compound **1** (1.5 mg) at 11 min.

The ES-B fraction was also passed through Diaion-HP (250–850 μm) column chromatography with H_2O to MeOH as the mobile phase, and seven major fractions (ES-B-1-1 ~ ES-B-1-7) were collected. Major fraction ES-B-1-3 (2.09 g) was subjected to C-18 column (75 μm, Nacalai Tesque, Kyoto, Japan) using H_2O to MeOH as the eluent, and 12 sub-fractions (ES-B-1-3-1 ~ ES-B-1-3-12) were collected. ES-B-1-3-10 was chromatographically purified by RP-HPLC column (Phenomenex Luna PFP, 5 μm, 10 × 250 mm) with 30% MeOH and at retention time of 15 min and flow rate 3 ml/min to collect compound **2** (2.8 mg). ES-B-1-3-11 was purified using RP-HPLC columns with 35% MeOH at 11 min and Phenomenex Luna PFP (5 μm, 10 × 250 mm) using 40% MeOH at a retention time of 11 min and a flow rate of 3 ml/min to collect compound **3** (3.1 mg).

2.2. Cell culture

We purchased primary human osteoblasts (HObs), osteoblast growth medium (OGM) and osteoblast differentiation medium (ODM) from Cell Applications (San Diego, USA). To obtain fully differentiated HOb cells, ODM, with dexamethasone, ascorbic acid and β-GP for mineralization was used, which is indicated as ODM miner hereafter (Imtiyaz et al., 2019; Mao et al., 2014). Puerarin was used as a positive control in this study, as it is reported to possess osteogenic potential (Wong and Rabie, 2007).

2.3. Cell viability analysis

HOb cells were seeded and treated with samples (isolated compounds at 100 μM and puerarin as the positive control at 1 μM) for five days. MTT assay was conducted to measure cell viability at an absorbance of 600 nm (Mao et al., 2014).

2.4. ALP activity

HOb cells (4×10^3/well) were seeded using OGM. The following day, OGM containing samples at various indicated concentrations was added and treated for three days. Following this cells were washed and lysed with PBS and 0.1% Triton X-100, respectively.

ALP activity was measured with *p*-nitrophenyl phosphate (dissolved in 6 mM sodium bicarbonate-sodium carbonate buffer, pH10.0) and bicinchoninic acid (BCA) protein using a BCA protein assay kit (Thermo Fisher Scientific), reaction was incubated at 37 °C for 1 h. After this ODs were measured and ALP activity was determined by normalizing ALP values to BCA values (Mao et al., 2014).

2.5. Alizarin red S staining

HOb cells were seeded using OGM, and 72 h later, samples were added. This was followed by the continuous treatment of samples in ODM miner every two days. After 11 days, mineralization assay was done according to Imtiyaz et al., 2019.

2.6. RNA isolation and real-time quantitative polymerase chain reaction

HOb cells were seeded using OGM, and the next day, samples were added. Cells were collected the following day and total cellular RNA was isolated using a High pure RNA isolation kit from Roche Life Science (Mannheim, Germany). In order to synthesize cDNA, a high-capacity cDNA reverse-transcription kit from Thermo Fisher Scientific was used.

A Roche™ Universal probe llibrary (UPL) probe and SYBR green master mix (Roche Life Science) including the SensiFAST™ probe no-ROX kit (Bioline, London, UK) were used for PCR amplification with the LightCycler® 480 system (Roche Life Science). Sequences of primers used are shown in Table 1. Gene expression levels were calculated by the $2^{(-\Delta\Delta Ct)}$ method, Livak formula, and normalized against GAPDH and expressed relative to the control (Imtiyaz et al., 2019).

2.7. Estrogen receptor (ER) expressions

HOb cells were seeded, and 24 h later OGM containing samples was added and treated for five days. Expression levels of ERs were detected using an ESR cell-based ELISA kit (Abnova, CA, USA) according to Imtiyaz et al. (2019).

2.8. Western blot analysis

HOb cells were seeded and 24 h later samples were added. After three days, cells were collected and lysed. Protein concentrations were measured and sodium dodecyl sulfate polyacrylamide gel electrophoresis was done to separate cell lysates. Lysates were transferred to polyvinylidene difluoride membranes, followed by probing with primary antibodies. Mouse anti-OPN and rabbit-anti TGF-β were purchased from GeneTex Inc. and were used at dilutions 1:1000. Rabbit anti-LC3I and LC3II were purchased from Thermo Fisher Scientific and were used at dilutions 1:1000. Rabbit anti-pSmad 1/5/8 were used at the dilutions of 1:500 and were purchased from Santa Cruz Biotechnology (CA, USA). Rabbit anti-β-actin was purchased from Abcam and was used at dilutions of 1:500. Secondary antibodies, goat anti-mouse IgG HRP from Thermo Fisher Scientific at 1:3000 and goat anti-rabbit IgG H&L HRP from Abcam at 1:3000 were used (Tai et al., 2020).

Table 1
Primer and probe combination used for the real-time PCR.

		Sequence (5′ → 3′)	Probe Number
Runx-2	Forward	CAGTGACACCATGTCAGCAA	41
	Reverse	GCTCACGTCGCTCATTTTG	
BMP-2	Forward	CGGACTGCGGTCTCCTAA	49
	Reverse	GGAAGCAGCAACGCTAGAAG	
BSP	Forward	GATTTCCAGTTCAGGGCAGT	63
	Reverse	TCTCCTTCATTTGAAGTCTCCTCT	
Col-1	Forward	AGGTCCCCCTGGAAAGAA	60
	Reverse	AATCCTCGAGCACCCTGA	
GAPDH	Forward	AGCCACATCGCTCAGACAC	60
	Reverse	GCCCAATACGACCAAATCC	
RANKL	Forward	CGTTGGATCACAGCACATCAG	n.a
	Reverse	GTACCAAGAGGACAGACTCAC	
OPG	Forward	CACTACTACACAGACAGCTGG	n.a
	Reverse	ACTCTATCTCAAGGTAGCGCC	

2.9. Statistical analysis

SigmaPlot version 11.0, developed by SYSTAT (IL, USA) was used to conduct all statistical analysis. The values represent mean ± standard deviation (S.D). A one-way analysis of variance (ANOVA) with Student-Newman-Keuls test was conducted and $p < 0.05$ was considered statistically significant.

3. Results

3.1. Isolation and identification of compounds

The ES extract was subjected to a series of chromatographic columns including Sepabox for separation, purification, and isolation. After using various spectroscopic techniques and literature comparison, we identified the isolated compounds to be syringaresinol (**1**) (Koul et al., 2016), syringin (**2**) (Ni et al., 2019), and (−)-epicatechin (**3**) (Fan et al., 2018) (Fig. 1).

3.2. Effect of syringin (*2*) and (−)-epicatechin (*3*) on the viability of HOb cells

Prior to analyzing the activity of the isolated compounds, their effect on cell viability was studied. Results showed that both **2** and **3** at 100 μM exerted negligible effect on the cell viability of HObs, as cell viability was above 80% (Fig. 2A).

3.3. Effect of syringin (*2*) and (−)-epicatechin (*3*) on ALP activity in HOb cells

ALP, a biomarker of bone formation and one of the key factors that directly induce deposition of minerals such as calcium and phosphate in bone (Mikami et al., 2016), was examined. Results showed that **2** increased ALP activity to 113.24% and 131.01% at 80 and 100 μM respectively. Similar results were observed wherein **3** significantly increased ALP activity to 111.17% and 130.67% at 80 and 100 μM, respectively. Taken together, these results showed that **2** and **3** concentration-dependently increased ALP activity to a similar degree (Fig. 2B).

3.4. Effect of syringin (*2*) and (−)-epicatechin (*3*) on mineral deposition in HOb cells

Mineralization is the quintessential outcome of bone formation in which mineral crystals are deposited in an organized manner onto the organic ECM (Boskey, 2007). Our results showed that **2** and **3**, even at the lowest doses tested, significantly increased mineral deposition in HOb cells. **2** at 60, 80, and 100 μM respectively increased mineralization to 112.05%, 125.32%, and 139.39%. Similar results were observed for **3** in which the increase in levels of mineralization was up to 116.83%, 127.87%, and 138.33% at 60, 80 and 100 μM, respectively (Fig. 3). These results demonstrated that both **2** and **3** induce mineralization in the HOb cells, and combined with the ALP activity results, indicate the osteogenic potentials of these compounds. We next sought to elucidate the potential underlying mechanism(s) through which these compounds induce bone formation.

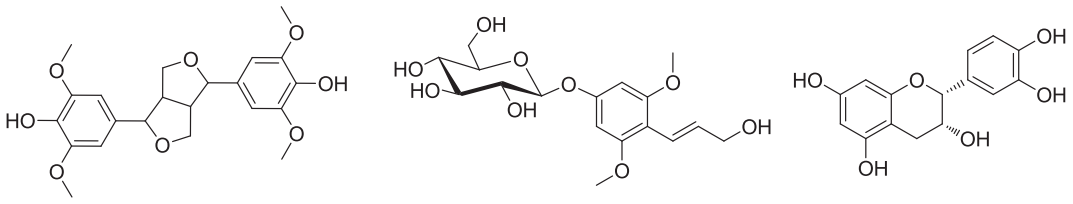

Fig. 1. Structure of compounds isolated from *E. spraguei.*

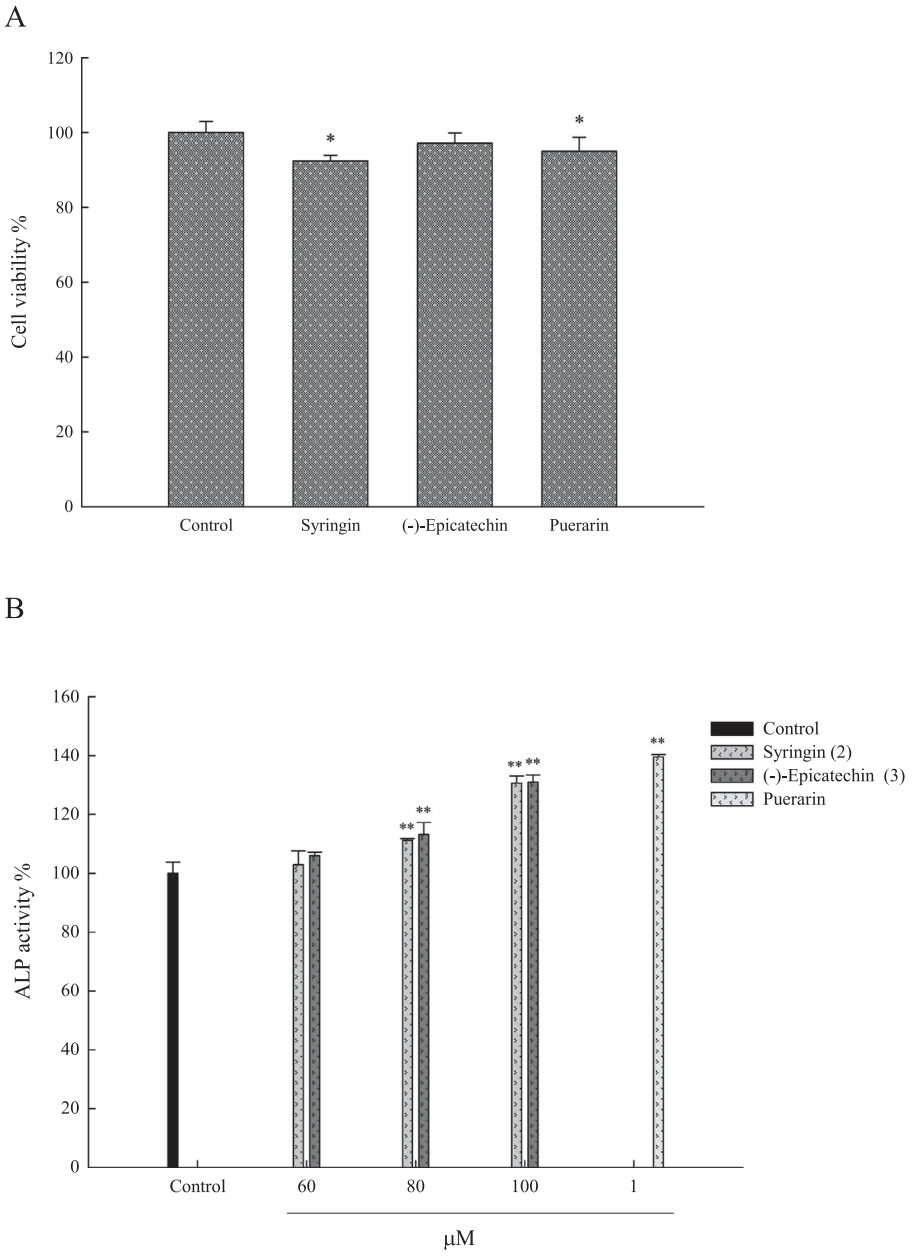

Fig. 2. Effect of syringin (**2**) and (−)-epicatechin (**3**) on the cell viability and ALP activity in HOb cells. Cells were seeded in 96-well plate and after 24 h samples were added using OGM. After 5 days (**A**) MTT was added and incubated for 4 h, after which cell viability was detected. (**B**) To analyze ALP activity, assay was performed and normalized by BCA. Results are from three independent repeats with errors bars indicating the mean ± standard deviation (SD), $^{*}p \leq 0.05$, $^{**}p \leq 0.01$ compared to the control.

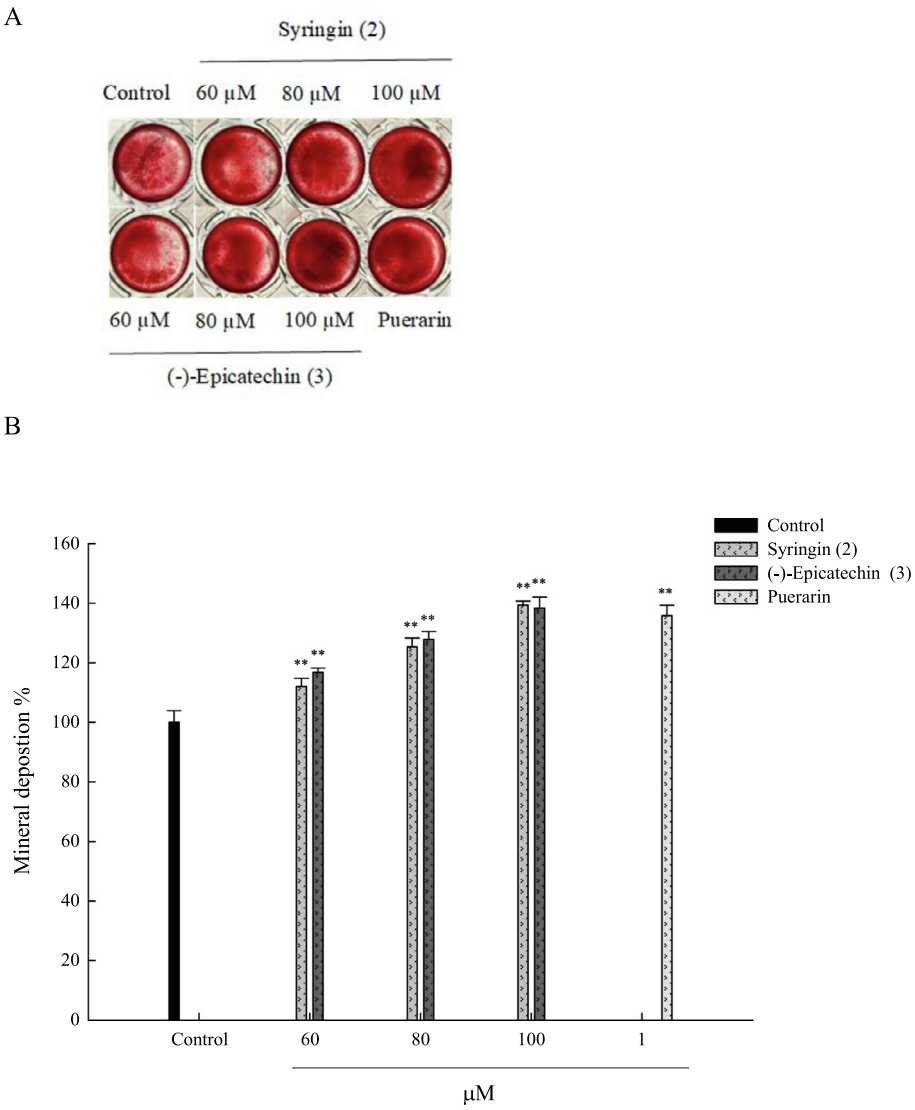

Fig. 3. Effect of syringin (**2**) and (−)-epicatechin (**3**) on mineral deposition in HOb cells. Cells were seeded in a 48-well plate and after 3 days, samples were added to cells using ODM miner. Following this samples at different doses with the promoter and inducer were added for the next 11 days using ODM miner. After that mineralization was detected using (**A**) Alizarin red staining and (**B**) quantification was done by de-staining. Results are from three independent repeats with errors bars indicating the mean ± standard deviation (SD), $^{**}p \leq 0.01$ compared to the control.

*3.5. Effect of syringin (**2**) and (−)-epicatechin (**3**) on expression of ERs in HOb cells*

ER-α is correlated with the bone mass in humans, as it is reported that the protection of cortical bone mass by estrogens is mediated via ER-α. Independent of estrogens, ER-α is also essential for bone formation, as it stimulates Wnt signaling (Khalid and Krum, 2016; Manolagas et al., 2013). However, ER-β works antagonistically to ER-α (Khalid and Krum, 2016). We examined the effect of **2** and **3** on expression levels of these receptors. Our results showed that 100 μM of **2** significantly increased the expression level of ER-α up to 113.42%, it also attenuated the expression of ER-β down to 91.99%. In contrast, **3** exerted no significant effect on the expression ER-α and -β (Fig. 4).

*3.6. Effect of syringin (**2**) and (−)-epicatechin (**3**) on expression levels of key genetic markers in HOb cells*

Bone formation is regulated by several genetic factors and signaling cascades. We examined the effect of isolated compounds (at 100 μM) on some key genes and transcription factors involved in the process of bone remodeling. Our results showed that **2** increased the mRNA expression levels of BMP-2, Col-1, BSP and Runx-2 up to 2.58, 1.43, 3.05 and 2.32 folds, respectively. The respective fold increase induced by **3** was up to1.93, 2.55, 1.58, and 1.68 for BMP-2, BSP, Col-1, and Runx-2 (Fig. 5A–D). In addition, **2** and **3** enhanced the mRNA expression levels of OPG/RANKL to 2.99 and 2.12 folds, respectively (Fig. 5E). These results demonstrated that **2** and **3** increased mRNA expression levels of several important genes implicated in bone formation, including BMP-2 pathway-associated genes (BMP-2, BSP, and Runx-2), suggesting that the osteogenic activity of these compound is mediated via the BMP-2 pathway.

*3.7. Effect of syringin (**2**) and (−)-epicatechin (**3**) on BMP-2 signaling in HOb cells*

To further substantiate the effect of the BMP-2 pathway in the osteogenic activity of the compounds, we conducted a Western blot analysis against BMP-2 pathway-associated proteins. Our

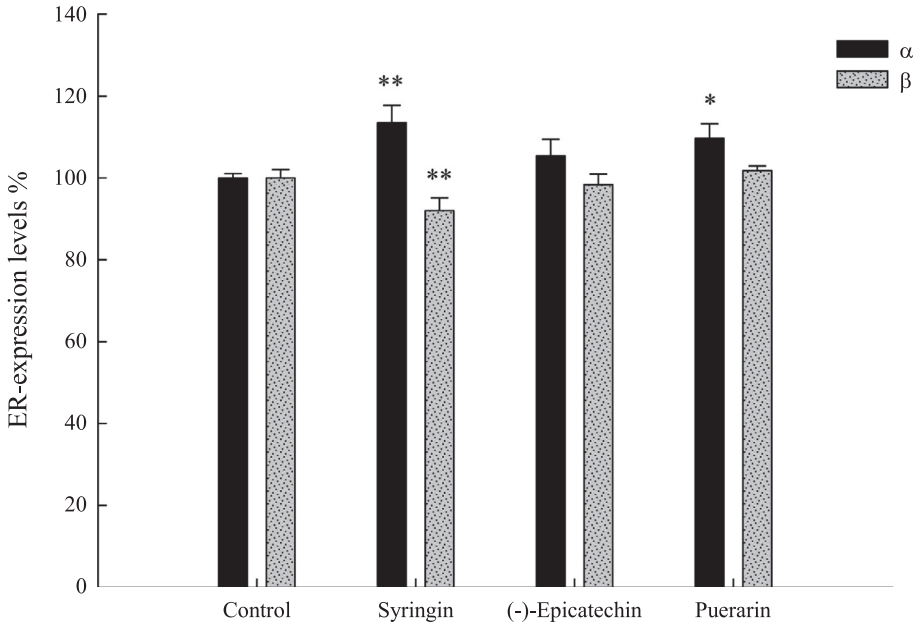

Fig. 4. Effect of syringin (**2**) on ERs. Cells were seeded in a 96-well plate and after 24 h, samples were added to cells using OGM. After 5 days, expression levels of estrogen receptors were detected by an ELISA using an ESR (Human) Cell-based ELISA kit from Abnova following the manufacturer's instructions. Results are from three independent repeats with errors bars indicating the mean ± standard deviation (SD), $^{*}p \leq 0.05$, $^{**}p \leq 0.01$ compared to the control.

results showed that at 100 μM, **2** and **3** significantly increased expression levels of BMP-2 pathway-associated proteins, TGF-β and pSmad 1/5/8 (Fig. 6A–C). To further confirm the involvement of BMP-2 in mediating osteogenic activity by **2** and **3**, we inhibited BMP-2 using the inhibitor dorsomorphin (20 μM for 72 h) and analyzed ALP activity. Results showed that in the presence of the inhibitor, levels of ALP activity dropped significantly, (Fig. 6D). Together, these results indicated that **2** and **3** induce osteogenesis through the BMP-2 pathway.

*3.8. Effect of syringin (**2**) and (−)-epicatechin (**3**) on autophagy in HOb cells*

Autophagy is essential for mineral deposition as studies have reported that loss of autophagy proteins resulted in decreased bone volume (Nollet et al., 2014). Once autophagy is induced, the essential autophagy protein microtubule-associated protein 1 light chain 3 (LC3I) becomes lipidated (LC3II). The conversation of LC3I to LC3II is the hallmark of autophagy. To examine if **2** and **3** (at 100 μM) modulate autophagy, we quantified protein levels of LC3II using Western blotting. Results showed that whereas **2** significantly induced autophagy, indicated by a substantial increase in LC3II expression, **3** decreased the expression of LC3II, indicating that **2**, but not **3**, induced autophagy (Fig. 7A and B). To understand the role of autophagy, we inhibited autophagy with bafilomycin (50 nM for 10 h), an inhibitor of autophagosome maturation. Results showed that inhibition of autophagy significantly decreased the **2**-mediated increase in ALP activity. In contrast, as expected, inhibition of autophagy did not significantly affect the **3**-mediated increase in ALP activity (Fig. 7C). These results showed that **2**, induces ALP activity also through the autophagy pathway.

*3.9. Effect of syringin (**2**) and (−)-epicatechin (**3**) on osteopontin (OPN) expression in HOb cells*

OPN, is an important non-collagenous protein that affects bone material properties and is involved in damage repair. Studies have shown that loss of OPN results in the loss of bone toughness, as it also regulates bone structure and morphology (Bailey et al., 2017; Bouleftour et al., 2016). We wanted to analyze if **2** and **3** at 100 μM regulate the expression level of OPN. Results showed that both **2** and **3** significantly upregulated OPN expression (Fig. 8).

4. Discussion

The process of bone remodeling involves the removal of old and damaged bone, followed by the formation of new bone. Any imbalance in this process result in the onset of disorders like osteopenia and osteoporosis (Katsimbri, 2017). These conditions are highly refractive to treatments due to clinically unmet needs. Plants and compounds derived from them possess medicinal potential for drug discovery against conditions like osteoporosis (Miller, 2016). Numerous studies have discovered that plants and their compounds can enhance bone formation (Gong et al., 2019; Yan et al., 2019). Our study is the first to introduce *Euonymus spraguei* as a plant that possesses osteogenic potential. In this study, we extracted stems of *E. spraguei* using 95% ethanol and isolated three compounds. The osteogenic potential of two of these isolated compounds was analyzed by examining their effect on biomarkers of bone formation. We also explored the possible underlying mechanisms responsible for their osteogenic potential by studying their interaction with various signaling pathways.

Syringin (**2**), is a phenolic glycoside belonging to eleutheroside derivatives. **2** was reported to possess certain pharmacological properties (Mahadeva Rao et al., 2015), including antioxidant activity (Kim et al., 2010; Liu et al., 2014), anti-diabetic effect (Krishnan et al., 2014), anti-allergic effect (Cho et al., 2001), protection against neuronal cell damage (Yang et al., 2010), anti-inflammatory effect (Cho et al., 2001; Choi et al., 2004), and inhibition of apoptosis (Yang et al., 2010). However, the osteogenic activity of **2** has not been extensively explored. A recent study reported that **2** prevented bone loss in ovariectomized mice by inhibiting osteoclastogenesis (Liu et al., 2018), without having any significant effect on ALP activity. In contrast to this study, we show here that **2** concentration-dependently induced ALP activity in HOb cells (Fig. 2B). The reason behind the varying results of

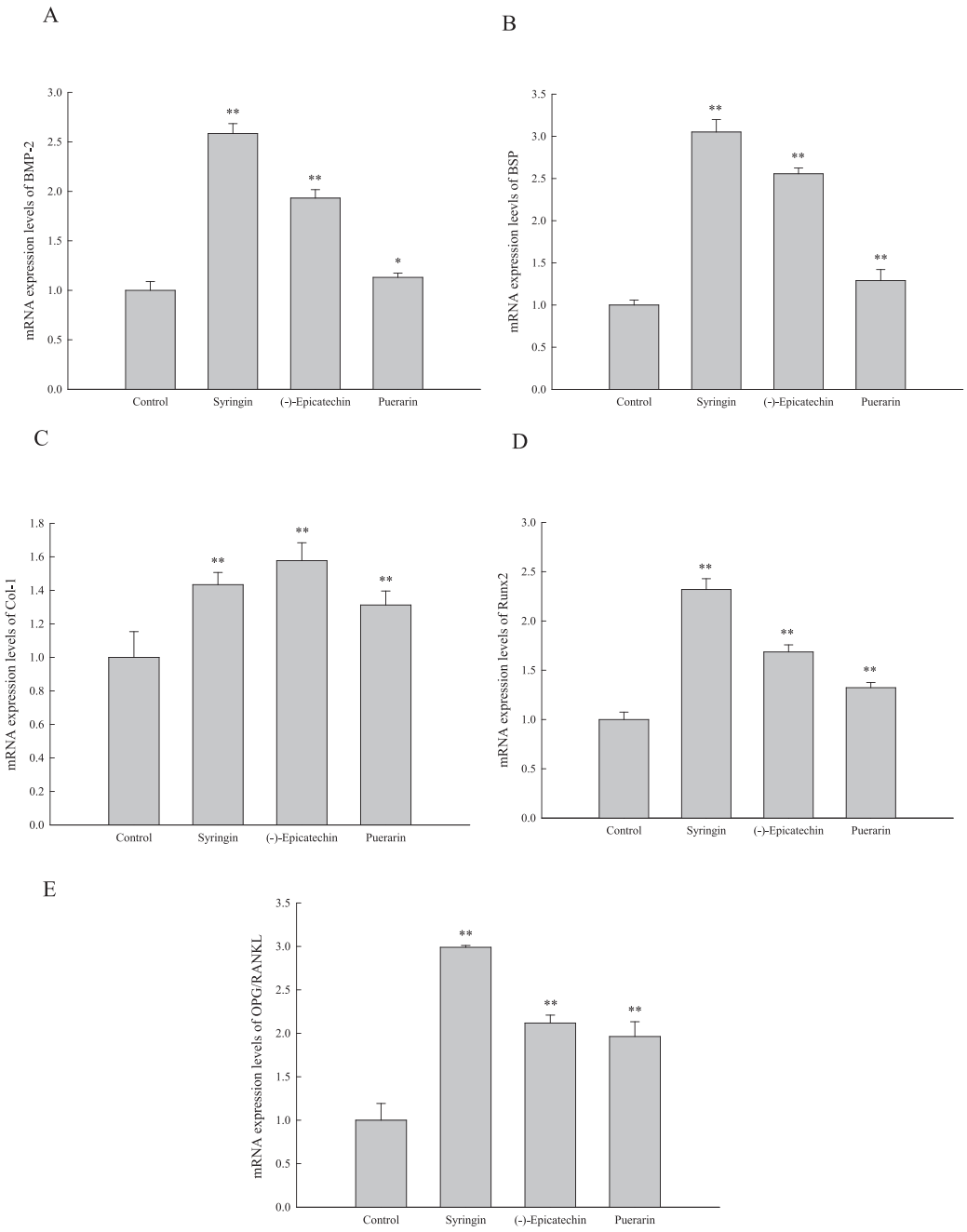

Fig. 5. Effect of syringin (**2**) and (−)-epicatechin (**3**) on bone formation-related genes HOb cells. Cells were seeded in 6-cm dishes and after 24 h, fresh ODM containing 100 μM of **2** and **3** was added. After 24 h cells were collected, followed by mRNA isolation and reverse transcription. Expression levels of (**A**) BMP-2, (**B**) BSP, (**C**) Col-1, (**D**) Runx2 and (**E**) OPG/RANKL were detected by performing a real-time PCR. Results are from three independent repeats with errors bars indicating the mean ± standard deviation (SD), $^{*}p \leq 0.05$, $^{**}p \leq 0.01$ compared to the control.

ALP activity could be due to differences in the experimental models, as other authors collected total protein from the bone of mice which included all bone cells whereas we analyzed ALP activity using HOb cells. Nonetheless, the finding that **2** can prevent osteoclastogenesis and enhance osteogenesis makes it an ideal starting-point material for development of a therapeutic strategy to enhance bone formation.

(−)-Epicatechin (**3**) belongs to the family of flavonoids that has diverse health benefits in humans. **3** also possesses numerous biological activities such as antitumor, antimicrobial, antioxidant, anti-inflammatory, neuroprotective and cardio protective activities (Prakash et al., 2019). A recent study reported that **3** rich *Marindo citrifolia* extract, ameliorated bone formation, strength and integrity in osteoarthritic rats through anti-inflammatory and anti-oxidative pathways (Wan Osman et al., 2019). Concordantly, our results indicated that **3** significantly increased ALP activity (Fig. 2B), a key biomarker of bone formation as well as the deposition of minerals in HOb cells (Fig. 3). Various derivatives and isomers of **3** have also been reported to enhance bone formation (Bakhsh et al., 2013), (−)-epicatechin-3-O-β-D-allopyranoside reduced arthritis severity score and prevented bone loss in collagen-induced arthritis mice (Hsiao et al., 2019). A study reported that (−)-epicatechin gallate stimulated osteoblast differentiation through Runx2 transcriptional activation

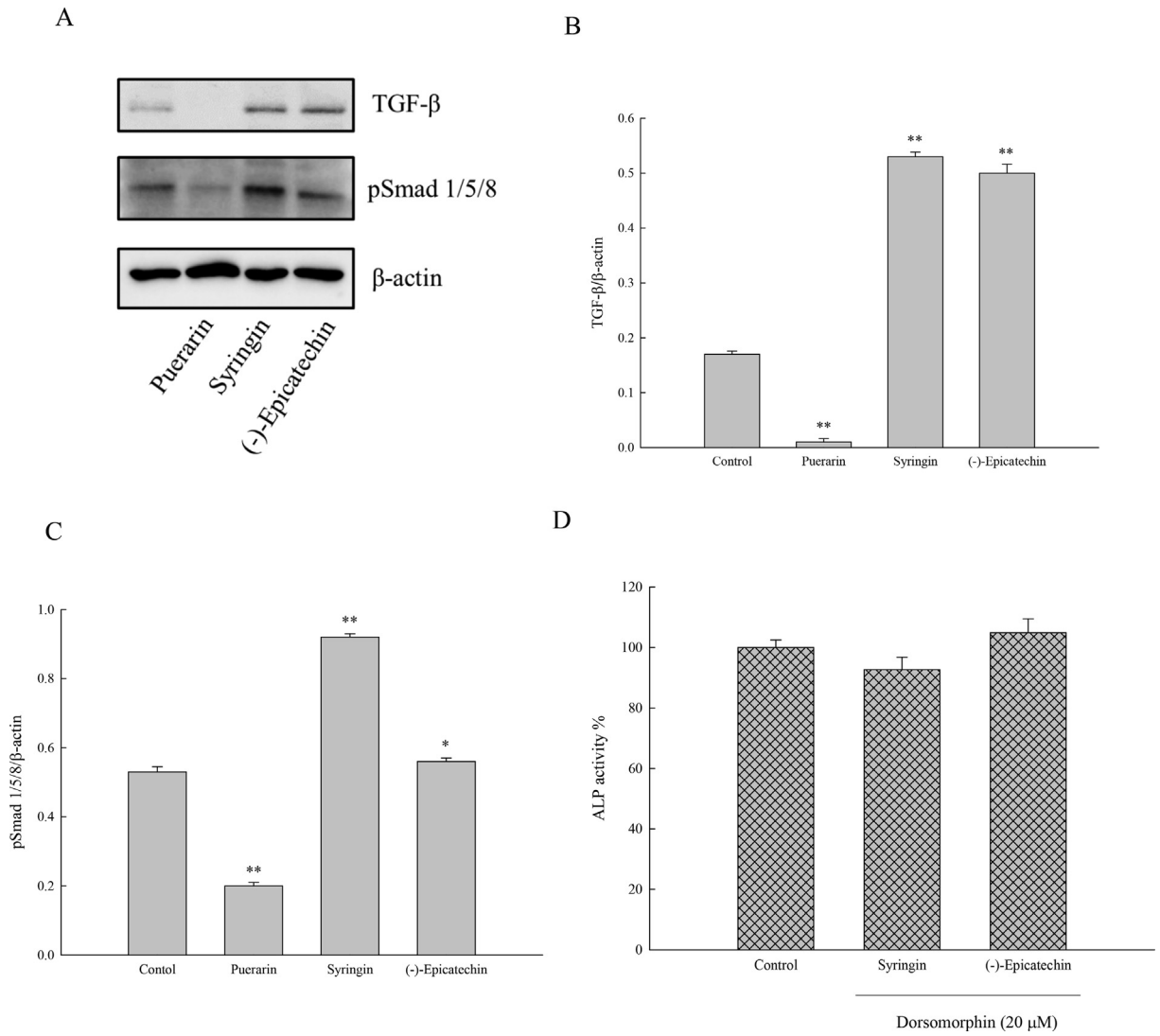

Fig. 6. Syringin (**2**) and (−)-epicatechin (**3**) mediates their effect *via* BMP-2 signaling pathway. Cells were seeded in 6 cm plates and after 24 hr treated with **2** and **3** at 100 μM for 3 days. (**A**) Cell lysates were collected and examined by a Western blot analysis to detect protein expression levels of TGF-β and pSmad 1/5/8. (**B** and **C**) Densitometry of A. To confirm that **2** and **3** mediate their osteogenic effect through the BMP-2 pathway we used the BMP-2 inhibitor, (**D**) dorsomorphin at 20 μM and analyzed its effect on ALP activity. Results are from three independent repeats with errors bars indicating the mean ± standard deviation (SD), $^{*}p \leq 0.05$, $^{**}p \leq 0.01$ compared to the control.

(Byun et al., 2014). Similarly, in our study, **3** significantly increased mRNA expression of Runx2, as well as BSP, a gene found downstream in the associated cascade (Fig. 5D and B). These results including our study clearly indicate the potential of **3** as bone formation-enhancing constituent.

BMP signaling plays an essential role in embryonic skeletal development as well as bone formation and homeostasis. BMP-2, a member of the BMP family is fundamental for osteoblast differentiation (Wu et al., 2016). A recent study showed that Guhong injection (GHI), a traditional compound preparation with **2** as one of its effective components, significantly increased BMP-2 and TGF-β expression levels (Sun et al., 2019). In parallel with that finding, we also showed that **2** and **3** enhanced expressions of BMP-2-associated proteins at both the mRNA (Fig. 5A, B and D) and protein levels (Fig. 6A and C). More importantly, pharmacological inhibition of BMP-2 activity significantly hampered **2**- and **3**-induced ALP activity (Fig. 6D), indicating the significance of the BMP-2 pathway in the osteogenic potential of these compounds. In agreement with our finding, Aoki et al. showed that BMP-2 is required for the induction of ALP activity (Aoki et al., 2001).

RANKL produced by osteoblasts on binding to its receptor RANK (present on osteoclast precursor cells), leads to the fusion of these cells, thereby forming multi-nucleated cells, which further differentiate into mature osteoblasts (Infante et al., 2019). However, a soluble decoy OPG produced by osteoblast binds to RANK, limiting excessive formation of mature osteoclasts (Martin and Sims, 2015). A study showed that **2** inhibited osteoclast formation (Li et al., 1998), and also prevented RANKL-induced osteoclast formation of bone marrow macrophages (Shim et al., 2015). This is in agreement with our study, as our results showed that both **2** and **3** increased the mRNA expression level of OPG and subsequently decreased the level of RANKL, thus elevating the OPG/RANKL ratio (Fig. 5E), which indicates inhibition of osteoclast differentiation and activation.

Autophagy is involved in osteoimmunology, bone homeostasis and mineralization (Nollet et al., 2014; Yin et al., 2019). SNPs in autophagy-related genes were found to directly influence the bone mineral density (Pan et al., 2010). Studies reported that deposition of minerals by BMP-2 in MC3T3-E1 cells significantly decreased in the presence of an autophagy inhibitor (Xu et al., 2019). Our results

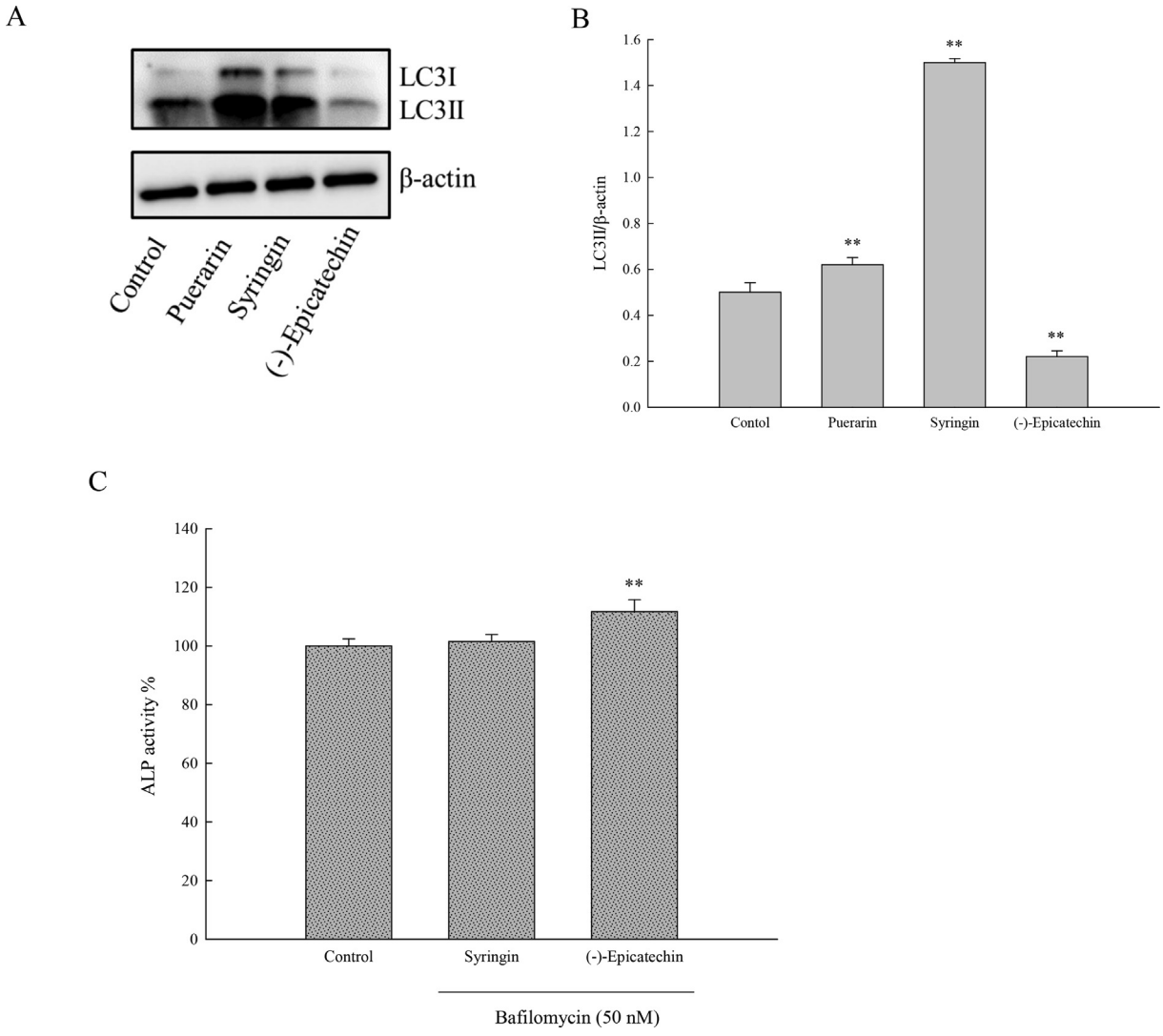

Fig. 7. Modulation of autophagy by syringin (**2**) and (−)-epicatechin (**3**) in HOb cells. Cells were seeded in 6 cm plates and after 24 h treated with **2** and **3** at 100 μM for 3 days. (**A**) Cell lysates were collected and examined by a Western blot analysis to detect protein expression levels of LC3I and LC3II. (**B**) Densitometry of A. To confirm the association of autophagy in the osteogenic potential of **2** and **3**, (**C**) autophagy was inhibited using bafilomycin (50 nM) and ALP activity was determined. Results are from three independent repeats with errors bars indicating the mean ± standard deviation (SD), $^{**}p \leq 0.01$ compared to the control.

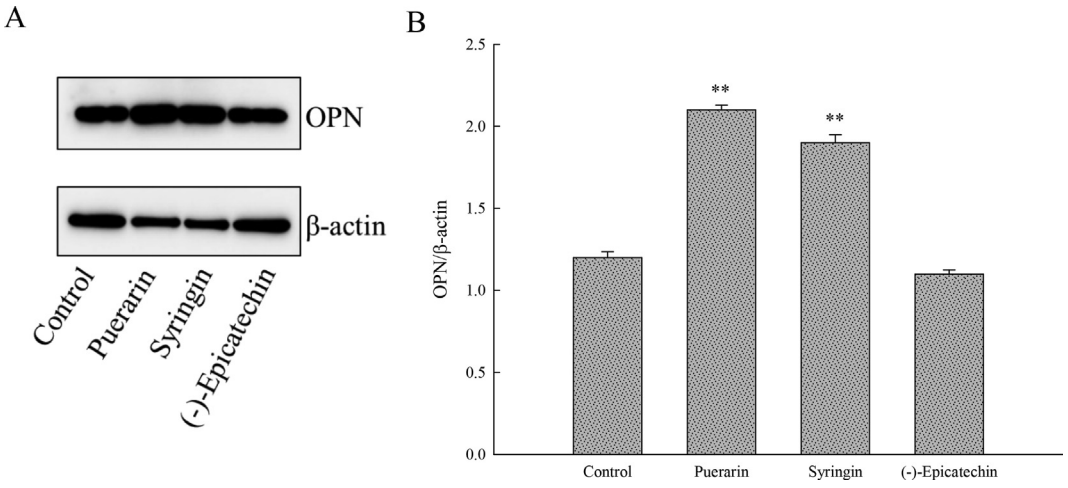

Fig. 8. Induction of OPN by syringin (**2**) and (−)-epicatechin (**3**) in HOb cells. Cells were seeded in 6 cm plates and after 24 h, were treated with **2** and **3** at 100 μM for 3 days. Cells lysates was collected and examined by a Western blot analysis to detect protein expression levels of (**A**) OPN (**B**) Densitometry of A. Results are from three independent repeats with errors bars indicating the mean ± standard deviation (SD), $^{**}p \leq 0.01$ compared to the control.

indicated that treatment with **2** robustly induced autophagy in HOb cells, as demonstrated by a significant increase in the LC3II level. Interestingly, in contrast to **2**, **3** inhibited autophagy in HOb cells (Fig. 7A and B). Consequently, inhibition of autophagy through bafilomycin treatment only attenuated **2**- but not 3-induced ALP activity (Fig. 7C). Precisely how autophagy enhances osteogenesis was unclear in a study by Nollet et al., 2014. However, a previous study done on osteoblast-like cells reported that inhibition of autophagy resulted in increased oxidative stress and stimulation of apoptosis, suggesting that autophagy attenuates oxidative stress and maintains cell survival (Yang et al., 2014). Given the role of autophagy in attenuating oxidative stress, it is plausible to speculate that autophagy could enhance osteogenesis by decreasing oxidative stress. Further research is needed to clarify the exact mechanism through which autophagy enhances osteogenesis in HOb cells.

5. Conclusions

Our study is the first to report isolation of compounds and pharmacological activity of *E. spraguei*. We showed that the active constituents, syringin (**2**) and (−)-epicatechin (**3**) obtained from *E. spraguei* elevated ALP activity and mineralization by targeting several pathways, including the ERs, BMP-2, and autophagy signaling. Our findings suggest that *E. spraguei* has osteogenic potential and its active agents can be considered for further investigations as MTD candidates for bone formation.

Funding

This study was funded by the Ministry of Science and Technology, Taiwan under grant number MOST106-2320-B-038-016-MY3.

Acknowledgements

The authors would like to thank Ih-Sheng Chen from Kaohsiung Medical University, the Instrumentation Center of National Taiwan University, and the Core Facility Center of Taipei Medical University.

Declaration of conflict of interest

The authors declared that there is no conflict of interest.

References

Alarcón, J., Cespedes, C.L., Muñoz, E., Balbontin, C., Valdes, F., Gutierrez, M., Astudillo, L., Seigler, D.S., 2015. Dihydroagarofuranoid sesquiterpenes as acetylcholinesterase inhibitors from Celastraceae Plants: *Maytenus disticha* and *Euonymus japonicus*. J. Agric. Food Chem. 63 (47), 10250–10256.

Aoki, H., Fujii, M., Imamura, T., Yagi, K., Takehara, K., Kato, M., Miyazono, K., 2001. Synergistic effects of different bone morphogenetic protein type I receptors on alkaline phosphatase induction. J. Cell Sci. 114 (8), 1483–1489.

Aubin, J.E., Triffitt, J.T., 2002. Mesenchymal stem cells and osteoblast differentiation. Principles of bone biology. Elsevier, 59–81.

Bailey, S., Karsenty, G., Gundberg, C., Vashishth, D., 2017. Osteocalcin and osteopontin influence bone morphology and mechanical properties. Ann. N.Y. Acad. Sci. 1409 (1), 79–84.

Bakhsh, A., Mustapha, N.M., Mohamed, S., 2013. Catechin-rich oil palm leaf extract enhances bone calcium content of estrogen-deficient rats. Nutrition 29 (4), 667–672.

Bolognesi, M.L., Cavalli, A., 2016. Multitarget drug discovery and polypharmacology. ChemMedChem 11 (12), 1190–1192.

Boskey, A.L., 2007. Mineralization of bones and teeth. Elements 3 (6), 385–391.

Bouleftour, W., Juignet, L., Bouet, G., Granito, R.N., Vanden-Bossche, A., Laroche, N., Aubin, J.E., Lafage-Proust, M.-H., Vico, L., Malaval, L., 2016. The role of the SIBLING, bone sialoprotein in skeletal biology — Contribution of mouse experimental genetics. Matrix Biol. 52–54 (5), 60–77.

Byun, M.R., Sung, M.K., Kim, A.R., Lee, C.H., Jang, E.J., Jeong, M.G., Noh, M., Hwang, E. S., Hong, J.H., 2014. (−)-Epicatechin gallate (ECG) stimulates osteoblast differentiation via Runt-related transcription factor 2 (RUNX2) and transcriptional coactivator with PDZ-binding motif (TAZ)-mediated transcriptional activation. J. Biol. Chem. 289 (14), 9926–9935.

Cha, B.Y., Park, C.J., Lee, D.G., Lee, Y.C., Kim, D.W., Kim, J.D., Seo, W.G., Kim, C.H., 2003. Inhibitory effect of methanol extract of *Euonymus alatus* on matrix metalloproteinase-9. J. Ethnopharmacol. 85 (1), 163–167.

Chang, B., Jin, C., Zhang, W., Kong, L., Yang, J.H., Lian, F.M., Li, Q.F., Yu, B., Liu, W.K., Yang, L.L., Zhao, P., Zhen, Z., 2012. *Euonymus alatus* in the treatment of diabetic nephropathy in rats. Am. J. Chin. Med. 40 (6), 1177–1187.

Cho, J.Y., Nam, K.H., Kim, A.R., Park, J., Yoo, E.S., Baik, K.U., Yu, Y.H., Park, M.H., 2001. In-vitro and in-vivo immunomodulatory effects of syringin. J. Pharm. Pharmacol. 53 (9), 1287–1294.

Choi, J., Shin, K.M., Park, H.J., Jung, H.J., Kim, H.J., Lee, Y.S., Rew, J.H., Lee, K.T., 2004. Anti-inflammatory and antinociceptive effects of sinapyl alcohol and its glucoside syringin. Planta Med. 70 (11), 1027–1032.

Compston, J.E., McClung, M.R., Leslie, W.D., 2019. Osteoporosis. Lancet 393 (10169), 364–376.

Fan, Y.C., Yue, S.J., Guo, Z.L., Xin, L.T., Wang, C.Y., Zhao, D.L., Guan, H.S., Wang, C.Y., 2018. Phytochemical composition, hepatoprotective, and antioxidant activities of *Phyllodium pulchellum* (L.). Desv. Mol. 23 (6), 1–15.

Gan, K., Xu, L., Feng, X., Zhang, Q., Wang, F., Zhang, M., Tan, W., 2015. Celastrol attenuates bone erosion in collagen-induced arthritis mice and inhibits osteoclast differentiation and function in RANKL-induced RAW264.7. Int. Immunopharmacol. 24 (2), 239–246.

Gong, W., Zhang, N., Cheng, G., Zhang, Q., He, Y., Shen, Y., Zhang, Q., Zhu, B., Zhang, Q., Qin, L., 2019. *Rehmannia glutinosa* Libosch extracts prevent bone loss and architectural deterioration and enhance osteoblastic bone formation by regulating the IGF-1/PI3K/mTOR pathway in streptozotocin-induced diabetic rats. Int. J. Mol. Sci. 20 (16), 1–18.

Hadjidakis, D.J., Androulakis, I.I., 2006. Bone remodeling. Ann. N.Y Acad. Sci. 1092, 385–396.

Hsiao, H.B., Wu, J.B., Lin, W.C., 2019. Anti-arthritic and anti-inflammatory effects of (−)-epicatechin-3-*O*-*β*-D-allopyranoside, a constituent of *Davallia formosana*. Phytomedicine 52, 12–22.

Imtiyaz, Z., Wang, Y.F., Lin, Y.T., Liu, H.K., Lee, M.H., 2019. Isolated compounds from *Turpinia formosana* Nakai induce ossification. Int. J. Mol. Sci. 20 (13), 1–17.

Infante, M., Fabi, A., Cognetti, F., Gorini, S., Caprio, M., Fabbri, A., 2019. RANKL/RANK/OPG system beyond bone remodeling: involvement in breast cancer and clinical perspectives. J. Exp. Clin. Cancer Res. 38 (1), 1–18.

Jimi, E., Hirata, S., Shin, M., Yamazaki, M., Fukushima, H., 2010. Molecular mechanisms of BMP-induced bone formation: Cross-talk between BMP and NF-κB signaling pathways in osteoblastogenesis. Jpn. Dent. Sci. Rev. 46 (1), 33–42.

Jolly, J.J., Chin, K.Y., Alias, E., Chua, K.H., Soelaiman, I.N., 2018. Protective effects of selected botanical agents on bone. Int. J. Environ. Res. Public Health 15 (5), 1–16.

Katsimbri, P., 2017. The biology of normal bone remodelling. Eur. J. Cancer Care 26 (6), 1–5.

Khalid, A.B., Krum, S.A., 2016. Estrogen receptors alpha and beta in bone. Bone 87 (6), 130–135.

Kim, S.J., Kim, Y.S., Kim, Y.C., 2010. Peroxyl radical scavenging capacity of extracts and isolated components from selected medicinal plants. Arch. Pharm. Res. 33 (6), 867–873.

Kobayashi, Y., Maeda, K., Takahashi, N., 2008. Roles of Wnt signaling in bone formation and resorption. Jpn. Dent. Sci. Rev. 44 (1), 76–82.

Koeberle, A., Werz, O., 2014. Multi-target approach for natural products in inflammation. Drug Discov. Today 19 (12), 1871–1882.

Koul, M., Meena, S., Kumar, A., Sharma, P.R., Singamaneni, V., Riyaz-Ul-Hassan, S., Hamid, A., Chaubey, A., Prabhakar, A., Gupta, P., Singh, S., 2016. Secondary metabolites from endophytic fungus *Penicillium pinophilum* induce ROS-mediated apoptosis through mitochondrial pathway in pancreatic cancer cells. Planta Med. 82 (4), 344–355.

Krishnan, S.S.C., Subramanian, I.P., Subramanian, S.P., 2014. Isolation, characterization of syringin, phenylpropanoid glycoside from *Musa paradisiaca* tepal extract and evaluation of its antidiabetic effect in streptozotocin-induced diabetic rats. Biomed. Prev. Nutr. 4 (2), 105–111.

Kusumoto, K., Bessho, K., Fujimura, K., Akioka, J., Okubo, Y., Wang, Y., Iizuka, T., Ogawa, Y., 2002. Osteoinduction by recombinant human bone morphogenetic protein-2 in muscles of non-human primates. J. Int. Med. Res. 30 (3), 251–259.

Li, H., Miyahara, T., Tezuka, Y., Namba, T., Nemoto, N., Tonami, S., Seto, H., Tada, T., Kadota, S., 1998. The Effect of kampo formulae on bone resorption *in vitro* and *in vivo*. I. Active constituents of Tsu-Kan-gan. Biol. Pharm. Bull. 21 (12), 1322–1326.

Liu, J., Zhang, Z., Guo, Q., Dong, Y., Zhao, Q., Ma, X., 2018. Syringin prevents bone loss in ovariectomized mice via TRAF6 mediated inhibition of NF-κB and stimulation of PI3K/AKT. Phytomedicine 42 (3), 43–50.

Liu, L.M., Cheng, S.F., Shieh, P.C., Lee, J.C., Chen, J.J., Ho, C.T., Kuo, S.C., Kuo, D.H., Huang, L.J., Way, T.D., 2014. The methanol extract of *Euonymus laxiflorus*, *Rubia lanceolata* and *Gardenia jasminoides* inhibits xanthine oxidase and reduce serum uric acid level in rats. Food Chem. Toxicol. 70 (8), 179–184.

Mahadeva Rao, U., Thant, Z., Muhammad, A., Bashir Ado, A., 2015. Chemistry and pharmacology of syringin, a novel biogycoside: A review. Asian J. Pharm. Clin. Res. 8 (3), 20–25.

Manolagas, S.C., O'Brien, C.A., Almeida, M., 2013. The role of estrogen and androgen receptors in bone health and disease. Nat. Rev. Endocrinol. 9 (12), 699–712.

Mao, Y.W., Lin, R.D., Hung, H.C., Lee, M.H., 2014. Stimulation of osteogenic activity in human osteoblast cells by edible *Uraria crinita*. J. Agric. Food Chem. 62 (24), 5581–5588.

Martin, T.J., Sims, N.A., 2015. RANKL/OPG; Critical role in bone physiology. Rev. Endocr. Metab. Disord. 16 (2), 131–139.

Medicine, U.S.N.L.o., 2018. Safety and efficacy study of ladostigil in mild to moderate probable Alzheimer's disease. https://clinicaltrials.gov/ct2/show/NCT01354691 (accessed 24 April, 2020).

Mikami, Y., Tsuda, H., Akiyama, Y., Honda, M., Shimizu, N., Suzuki, N., Komiyama, K., 2016. Alkaline phosphatase determines polyphosphate-induced mineralization in a cell-type independent manner. J. Bone Miner. Metabol. 34 (6), 627–637.

Miller, P.D., 2016. Management of severe osteoporosis. Expert Opin. Pharmacol. 17 (4), 473–488.

Morphy, R., 2010. Selectively nonselective kinase inhibition: Striking the right balance. J. Med. Chem. 53 (4), 1413–1437.

Nguyen, V.B., Nguyen, A.D., Nguyen, Q.V., Wang, S.L., 2017a. Porcine pancreatic α-amylase inhibitors from *Euonymus laxiflorus* Champ. Res. Chem. Intermediat. 43 (1), 259–269.

Nguyen, V.B., Nguyen, Q.V., Nguyen, A.D., Wang, S.L., 2017b. Screening and evaluation of α-glucosidase inhibitors from indigenous medicinal plants in Dak Lak Province, Vietnam. Res. Chem. Intermediat. 43 (6), 3599–3612.

Nguyen, V.B., Wang, S.L., Nguyen, A.D., Lin, Z.H., Doan, C.T., Tran, T.N., Huang, H.T., Kuo, Y.H., 2019. Bioactivity-guided purification of novel herbal antioxidant and anti-NO compounds from Euonymus laxiflorus Champ. Molecules 24 (1), 112–120.

Ni, J.C., Shi, J.T., Tan, Q.W., Chen, Q.J., 2019. Two new compounds from the fruit of *Ailanthus altissima*. Nat. Prod. Res. 33 (1), 101–107.

Nishimura, R., Hata, K., Ikeda, F., Ichida, F., Shimoyama, A., Matsubara, T., Wada, M., Amano, K., Yoneda, T., 2008. Signal transduction and transcriptional regulation during mesenchymal cell differentiation. J. Bone Miner. Metab. 26 (3), 203–212.

Nollet, M., Santucci-Darmanin, S., Breuil, V., Al-Sahlanee, R., Cros, C., Topi, M., Momier, D., Samson, M., Pagnotta, S., Cailleteau, L., 2014. Autophagy in osteoblasts is involved in mineralization and bone homeostasis. Autophagy 10 (11), 1965–1977.

Pan, F., Liu, X.G., Guo, Y.F., Chen, Y., Dong, S.S., Qiu, C., Zhang, Z.X., Zhou, Q., Yang, T. L., Guo, Y., 2010. The regulation-of-autophagy pathway may influence Chinese stature variation: evidence from elder adults. J. Hum. Genet. 55 (7), 441–447.

Prakash, M., Basavaraj, B.V., Chidambara Murthy, K.N., 2019. Biological functions of epicatechin: Plant cell to human cell health. J. Funct. Foods 52 (12), 14–24.

Raggatt, L.J., Partridge, N.C., 2010. Cellular and molecular mechanisms of bone remodeling. J. Biol. Chem. 285 (33), 25103–25108.

Ramsay, R.R., Popovic-Nikolic, M.R., Nikolic, K., Uliassi, E., Bolognesi, M.L., 2018. A perspective on multi-target drug discovery and design for complex diseases. Clin. Transl. Med. 7 (1), 1–14.

Rizzoli, R., Reginster, J.Y., Boonen, S., Bréart, G., Diez-Perez, A., Felsenberg, D., Kaufman, J.M., Kanis, J.A., Cooper, C., 2011. Adverse reactions and drug-drug interactions in the management of women with postmenopausal osteoporosis. Calcif. Tissue. Int. 89 (2), 91–104.

Sams-Dodd, F., 2005. Target-based drug discovery: is something wrong?. Drug Discov. Today 10 (2), 139–147.

Shao, J., Wang, H., Hu, X., 2016. Antioxidant activities of the total flavonoids from the horticulture plant of *Euonymus fortunei* Hand. leaves. Tianjin Agric. Sci. 1 (10), 37–41.

Sharma, A., Chandra Sati, S., Prakash Sati, O., Dhobhal Sati, M., Kumar Kothiyal, S., 2012. Genus *Euonymus*: chemical and pharmacological perception. Mini-Rev. Org. Chem. 9 (4), 341–351.

Shim, K.S., Kim, T., Ha, H., Lee, C.J., Lee, B., Kim, H.S., Park, J.H., Ma, J.Y., 2015. Water extract of *Magnolia officinalis* cortex inhibits osteoclastogenesis and bone resorption by downregulation of nuclear factor of activated T cells cytoplasmic 1. Integr. Med. Res. 4 (2), 102–111.

Sun, C.R., Hu, H.J., Xu, R.S., Yang, J.H., Wan, H.T., 2009. A new friedelane type triterpene from *Euonymus hederaceus*. Molecules 14 (7), 2650–2655.

Sun, Z., Jin, H., Zhou, H., Yu, L., Wan, H., He, Y., 2019. Guhong Injection promotes fracture healing by activating Wnt/beta-catenin signaling pathway *in vivo* and *in vitro*. Biomed. Pharmacother. 120 (9), 1–10.

Tai, C.J., Jassey, A., Liu, C.H., Tai, C.J., Richardson, C.D., Wong, S.H., Lin, L.T., 2020. Targeting autophagy augments BBR-mediated cell death in human hepatoma cells harboring hepatitis C virus RNA. Cells 9 (4), 1–18.

Van der Schyf, C.J., 2011. The use of multi-target drugs in the treatment of neurodegenerative diseases. Expert Rev. Clin. Pharmacol. 4 (3), 293–298.

Wan Osman, W.N., Che Ahmad Tantowi, N.A., Lau, S.F., Mohamed, S., 2019. Epicatechin and scopoletin rich Morinda citrifolia (Noni) leaf extract supplementation, mitigated osteoarthritis via anti-inflammatory, anti-oxidative, and anti-protease pathways. J. Food Biochem. 43 (3).

Wei, Q., Liu, J., 2016. Chemical components of the essential oils of leaf, stem and fruit from *Euonymus japonicus* Thunb. and their antiviral activities. Chin. J. App. Chem. 33 (6), 719–726.

Wong, R., Rabie, B., 2007. Effect of puerarin on bone formation. Osteoarthr. Cartil. 15 (8), 894–899.

Wu, M., Chen, G., Li, Y.P., 2016. TGF-β and BMP signaling in osteoblast, skeletal development, and bone formation, homeostasis and disease. Bone Res. 4 (1), 1–21.

Xu, X., Sun, M., Wang, D., Bu, W., Wang, Z., Shen, Y., Zhang, K., Zhou, D., Yang, B., Sun, H., 2019. Bone formation promoted by bone morphogenetic protein-2 plasmid-loaded porous silica nanoparticles with the involvement of autophagy. Nanoscale 11 (45), 21953–21963.

Yan, C., Zhang, S., Wang, C., Zhang, Q., 2019. A fructooligosaccharide from A*chyranthes bidentata* inhibits osteoporosis by stimulating bone formation. Carbohydr. Polym. 210 (1), 110–118.

Yang, E.J., Kim, S.I., Ku, H.Y., Lee, D.S., Lee, J.W., Kim, Y.S., Seong, Y.H., Song, K. S., 2010. Syringin from stem bark of *Fraxinus rhynchophylla* protects Aβ (25–35)-induced toxicity in neuronal cells. Arch. Pharmacal. Res. 33 (4), 531–538.

Yang, Y.H., Li, B., Zheng, X.F., Chen, J.W., Chen, K., Jiang, S.D., Jiang, L.S., 2014. Oxidative damage to osteoblasts can be alleviated by early autophagy through the endoplasmic reticulum stress pathway—implications for the treatment of osteoporosis. Free Radic. Biol. Med. 77, 10–20.

Yang, Y., Gu, L., Xiao, Y., Liu, Q., Hu, H., Wang, Z., Chen, K., 2015. Rapid identification of α-glucosidase inhibitors from *Phlomis tuberosa* by Sepbox chromatography and thin-layer chromatography bioautography. PLOS ONE 10 (2), 1–13.

Yin, X., Zhou, C., Li, J., Liu, R., Shi, B., Yuan, Q., Zou, S., 2019. Autophagy in bone homeostasis and the onset of osteoporosis. Bone Res. 7 (1), 1–28.